

Aniruddha Agarwal and Vishali Gupta

Abstract

Systemic infectious diseases can affect various organ systems including the ocular tissue. Organisms such as bacteria, viruses, fungi, and parasites can disseminate from their systemic foci of infection and involve the retinal and the choroid. Retinochoroidal involvement due to systemic infectious conditions can present with protean clinical manifestations and can often result in a diagnostic challenge. Often, these entities can present with unusual ocular findings. Thus, the clinician may need advanced laboratory support including analysis of ocular fluids and/or tissues to establish accurate diagnosis. In the past few decades, there have been numerous advances in the field of ocular imaging. With the introduction of newer imaging modalities such as enhanced-depth imaging optical coherence tomography and ultrawide-field fundus photography, it is possible to obtain high-quality near-histological images of the retina and choroid. Such observations can greatly aid the clinician in establishing the diagnosis early. In the index chapter, infectious chorioretinal diseases such as tuberculosis, toxoplasmosis, Lyme disease, and syphilis have been described with an emphasis on their clinical and imaging features.

A. Agarwal

Department of Ophthalmology, Advanced Eye Center, Post Graduate Institute of Medical Education and Research (PGIMER), Sector 12, Chandigarh 160012, India

V. Gupta (✉)

Department of Ophthalmology, Advanced Eye Center, Post Graduate Institute of Medical Education and Research (PGIMER), Sector 12, Chandigarh 160012, India

e-mail: vishalisara@yahoo.co.in

9.1 Introduction

A number of systemic infections can result in ocular disease that may be associated with severe visual morbidity. Often, ocular findings may be the presenting feature of these conditions. On the other hand, delay in the diagnosis of infectious posterior uveitis and chorioretinitis may be associated with permanent visual impairment [1]. While systemic infections caused by bacteria, viruses, fungi, and parasites are more common in developing countries, many pathogens are endemic throughout the world, and thus, conditions such as tuberculosis can present in developed countries as well [2]. Therefore, a clinician must rule out infectious etiologies when evaluating every case of chorioretinitis because immunosuppressive therapy in the absence of appropriate antibiotic cover can lead to life-threatening fulminant disease. In addition, ocular infection can rapidly spread resulting in sight-threatening sequelae.

Apart from direct invasion of the ocular tissues, systemic infectious agents can result in retinochoroidal inflammation due to altered immunological response of the host due to various mechanisms such as molecular mimicry [3]. Hypersensitivity reaction to the proteins of such infectious microorganisms can also result in tissue damage and inflammation. Thus, immunological response of the host plays an important role in pathogenesis of the disease.

With advancing biomedical engineering techniques, a number of state-of-the-art imaging devices have been introduced in the field of ophthalmology in the past few decades. It is now possible to image various ocular tissues noninvasively.

With the help of multimodal imaging techniques, staging, treatment response, and prognosis of various entities such as tubercular serpiginous-like choroiditis (SLC) and toxoplasmosis can be accurately assessed. In the following sections, a comprehensive overview of imaging features for each of these conditions is presented.

9.2 Tuberculosis

Tuberculosis (TB) is a leading infectious cause of morbidity and mortality. Worldwide, one-third of the population is estimated to be infected with *Mycobacterium tuberculosis* (*latent TB*). Nearly 10% of individuals with latent TB are likely to develop the disease at some time in their lives [4]. In 2014, 9.6 million individuals the world over suffered from TB-related disease with over 1.5 million TB-related deaths [5]. During the same year, the rate of decline of TB cases decreased in the USA, suggesting that the disease may potentially reemerge even in non-endemic areas.

9.2.1 Systemic Features of Tuberculosis

The spread of TB occurs through the aerial route. When infectious mycobacteria are inhaled, primary infection may occur in the lung. Involvement of lung parenchyma, regional lymph nodes, and pleural tissue may result in the formation of *Ghon focus*. If the host's immune system is capable of destroying the multiplying mycobacteria,

the patient may not manifest the disease. However, reactivation of the disease is possible in the future during states of immunosuppression. Pulmonary TB may present with cavitary lesions and destruction of lung parenchymal tissue. Pleural effusion may accompany lesions in the lung [6].

Dissemination of the organism may occur and extrapulmonary sites may be affected due to TB. Commonly affected organs include the central nervous system (*tubercular meningitis*), cardiovascular system, liver, gastrointestinal system, vertebrae (*Pott's spine*), joints (*tubercular arthritis*), and lymph nodes, among others. Extrapulmonary involvement with TB may be very severe, especially in the presence of HIV coinfection [7]. Highly virulent form of the disease may ensue, leading to rapid weight loss, wasting, and death of the patient [8].

9.2.2 Intraocular Tuberculosis

Intraocular TB represents an extrapulmonary form of the disease, which may occur in 1.4–6.8% of patients with pulmonary TB [9, 10]. However, often intraocular TB may not be accompanied by pulmonary disease making the diagnosis challenging. Moreover, the paucibacillary nature of ocular infection makes the microbiological diagnosis challenging [11]. Therefore, diagnosis of intraocular TB is based on a multitude of clinical findings, systemic TB, chorioretinal imaging, and supportive laboratory tests evaluating tubercular hypersensitivity (such as tuberculin skin test and interferon gamma release assay).

Although posterior segment uveitis is the most common form of intraocular TB, patients may present with chronic, recurrent anterior uveitis. Anterior uveitis is usually granulomatous inflammation with cells, flare, rarely hypopyon, mutton-fat keratic precipitates, iris nodules (Koeppel's or Busacca's), and broad-based posterior synechiae. TB-related granulomas may be found in the angle of the anterior chamber. Chronic anterior uveitis may be associated with development of posterior subcapsular cataract, pupillary block, and secondary glaucoma. Other features include iris neovascularization and band-shaped keratopathy. Intermediate uveitis may be seen due to spillover of the inflammation into the vitreous cavity. There may be severe vitritis, snow balls, snow banking, peripheral vascular sheathing, and cystoid macular edema. There may be presence of tuberculomas of the ciliary body detectable on ultrasound biomicroscopy [11].

Posterior segment manifestations of ocular TB include *serpiginous-like choroiditis* (or *multifocal serpiginous choroiditis*), tubercular granulomas or tubercles, subretinal abscesses, neuroretinitis, retinal vasculitis, and rarely endophthalmitis or panophthalmitis [2, 11, 12]. The following sections describe clinical and imaging characteristics of tubercular lesions that primarily involve the retinochoroid.

9.2.2.1 Serpiginous-Like Choroiditis

Serpiginous-like choroiditis (SLC) typically affects young to middle-aged adults from TB-endemic areas (Fig. 9.1) [13, 14]. Unlike autoimmune serpiginous choroiditis, tubercular serpiginous-like choroiditis occurs at a younger age, associated

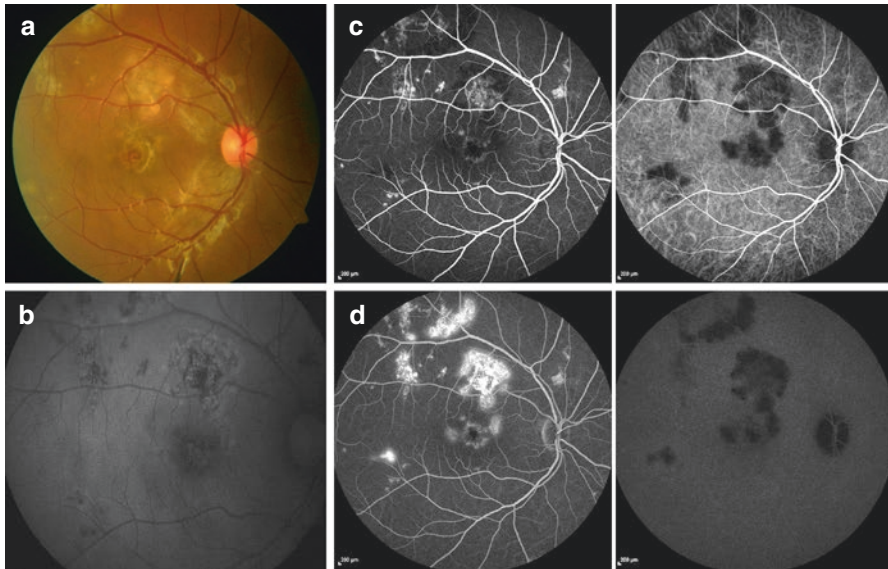


Fig. 9.1 Multimodal imaging of a 24-year-old male diagnosed with tubercular serpiginous-like choroiditis (SLC). (a) Color fundus photography shows presence of multifocal yellowish-white perivascular choroiditis lesions involving the posterior pole and mid-periphery. On fundus autofluorescence, the lesions show central areas of hypo-autofluorescence. Active edges appear hyper-autofluorescent (b). Simultaneous fluorescein angiography (FA) and indocyanine green angiography (ICGA) in the early phase (c) show RPE window defects in the healed areas. Active lesions appear hypofluorescent on FA. ICGA shows diffuse hypofluorescence. In the late phase (d), the active lesions show intense hyperfluorescence on FA and hypofluorescence on ICGA

with mild vitritis, and is bilateral in majority of the cases [15]. TB SLC may have different morphological patterns [13]:

1. Multifocal choroiditis: This phenotype presents with discreet lesions, is yellowish white in color, measures about $\frac{1}{4}$ –1 disk diameter in size with well-defined margins and slightly raised edges which are noncontiguous to begin with, and shows a wavelike progression over a period of 1–4 weeks and gradually becomes confluent (Fig. 9.1).
2. Placoid chorioretinitis: This phenotype presents with a diffuse plaque-like lesion with an amoeboid pattern and active serpiginous-like edge at the initial presentation. The edges are yellowish white and elevated, whereas the center of the lesion is less elevated with pigmentary changes suggestive of a healing process in the center of the lesion.
3. Mixed pattern: These lesions present with overlapping features of both multifocal and placoid chorioretinitis.

9.2.2.2 Choroidal Granulomas, Tubercles, and Subretinal Abscesses

Choroidal granulomas and tubercles occur as a result of hematogenous dissemination of TB bacilli from pulmonary and extrapulmonary sites [2, 16]. The tubercles may be unilateral or bilateral, usually multiple, discreet grayish-white to yellowish subretinal lesions with indistinct borders. The lesions are usually seen in the posterior pole but may be present in the mid-periphery [10]. A choroidal granuloma may clinically resemble non-inflammatory condition such as central serous chorioretinopathy, choroidal metastases, melanoma of the choroid, and age-related macular degeneration (Fig. 9.2).

On the other hand, solitary choroidal granuloma may present as a large, elevated yellowish *subretinal mass* often associated with exudative retinal detachment. The lesion is associated with rapid necrosis and tissue destruction [17]. These patients often have disseminated systemic TB [18]. TB-related subretinal abscess appears distinct and more yellowish in color compared to a small choroidal granuloma. They usually have overlying retinal hemorrhages and have a tendency to develop retinal angiomatous proliferation over a period of time.

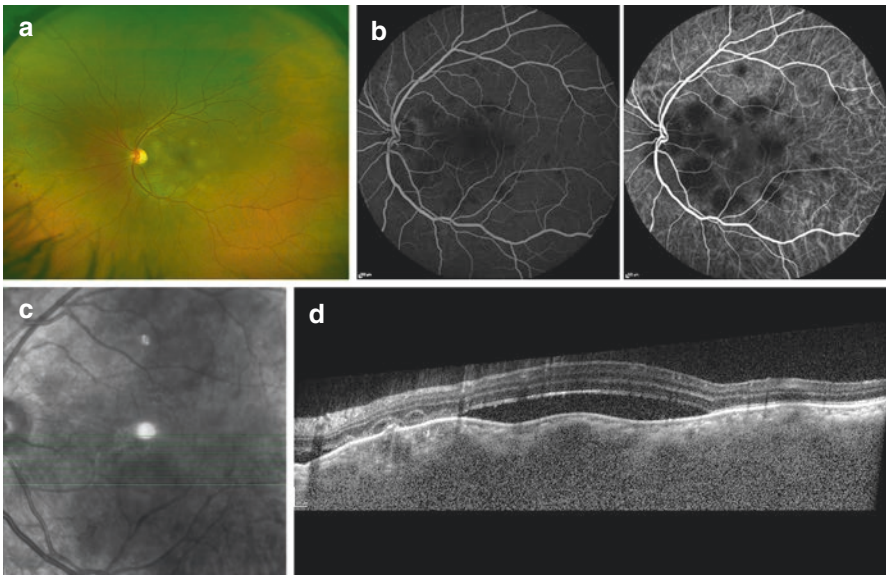


Fig. 9.2 Imaging features of a 40-year-old male with tubercular granulomas in the *left* eye. On ultrawide-field fundus photography (a), the lesions appear yellow-white, subretinal, and multiple, involving the posterior pole. Simultaneous fluorescein angiography (FA) and indocyanine green angiography (ICGA) in the early phase (b) show hypofluorescence of the lesions. On infrared imaging (c), the granulomas are clearly demarcated. Enhanced-depth imaging optical coherence tomography through the subretinal granuloma shows elevation of RPE due to the granulomas, subretinal fluid, and atrophy of the inner choroidal vasculature (d)

9.2.2.3 Tubercular Retinitis

Rarely, intraocular TB may present with atypical features mimicking other etiologies of infectious necrotizing retinitis such as viral (herpetic) retinitis or atypical toxoplasma retinochoroiditis. Often, these patients may be immunocompromised due to HIV coinfection. Such cases may be accompanied by retinal periphlebitis [19].

9.2.3 Imaging Features

9.2.3.1 Fundus Photography, Autofluorescence, and Ultra-wide field Fundus Imaging

Since the diagnosis of TB SLC depends upon the clinical appearance and morphology of the choroiditis lesions, adequate assessment of the disease phenotype using high-quality color fundus photography is essential. Serial fundus photography (from acute stage to the stage of healing) is very useful in the assessment of morphological evolution of the lesions [13]. In addition, color fundus photography can enable detection of vitreous haze among patients with intraocular TB.

FAF is a very useful noninvasive imaging modality in the management of TB SLC. Characteristic changes are observed on FAF as the lesions evolve from active to healed stage. Lesions of TB SLC can be staged using FAF to determine the response of therapy (Fig. 9.3) [20]. Active lesions demonstrate ill-defined hyper-autofluorescence throughout the lesions giving them a diffuse, amorphous appearance (stage 1). In the stage of early healing, a thin rim of hypo-autofluorescence is seen surrounding the lesion which remains predominantly hyper-autofluorescent with a stippled pattern (stage 2). With further healing, the lesion becomes predominantly hypo-autofluorescent (stage 3). On complete healing, the lesions become uniformly hypo-autofluorescent (stage 4) (Fig. 9.3; Table 9.1) [20].

Ultrawide-field fundus imaging can provide new insights into the disease pathophysiology. In a recent study, using ultrawide-field imaging, additional features such as peripheral choroiditis, active retinal vasculitis, and neovascularization were observed among patients with TB SLC compared to conventional imaging [21]. Using this technology, it is possible to simultaneously document posterior and peripheral TB SLC lesions in one image and monitor the overall response to treatment on successive visits. Therefore, ultrawide-field imaging may be superior to conventional imaging in identifying changes such as *peripheral paradoxical worsening* which may be otherwise missed (Fig. 9.4) [21].

9.2.3.2 Fluorescein Angiography

On FA, active lesions of TB SLC are hypofluorescent in the early phase. Active lesions show late hyperfluorescence. As the lesions progress and become confluent, the advancing edge shows early hypofluorescence with late hyperfluorescence. Areas of resolution show retinal pigment epithelial transmission defects. Choroidal tubercles and granulomas are hypofluorescent in the phase of early dye transit and become hyperfluorescent in the late frames (Fig. 9.1) [13].

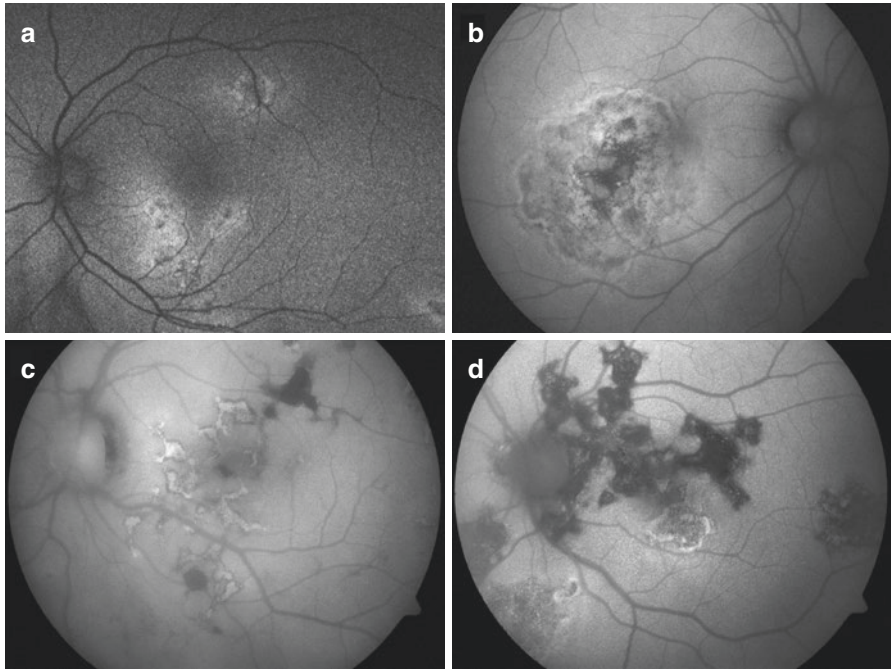


Fig. 9.3 Fundus autofluorescence of tubercular serpiginous-like choroiditis (SLC) lesions in various stages of the disease. In the early active stage (a), there is diffuse hyper-autofluorescence of the lesions (stage 1). Stage 2 is characterized by a thin rim of hypo-autofluorescence surrounding the hyper-autofluorescent lesions (b). Stage 3 is characterized by stippled appearance with mixed hyper- and hypo-autofluorescence, but predominant hypo-autofluorescence (c). In the stage 4, the lesions appear uniformly hypo-autofluorescent (d)

Ultrawide-field FA is very useful in the management of intraocular TB. In comparison with conventional FA, ultrawide-field imaging can reveal additional information such as peripheral capillary non-perfusion areas, retinal neovascularization, and retinal vascular leakage. Such findings may alter treatment decisions such as the need for scatter laser photocoagulation [21].

9.2.3.3 Indocyanine Green Angiography

Active lesions of TB SLC remain hypofluorescent from early to late phase on ICGA. ICGA is very useful in detecting choriocapillaritis among patients with tubercular choroiditis. On the other hand, choroidal tubercles show early and intermediate hypofluorescence on ICGA. In the late phase, the lesions may become hyperfluorescent (type 1) indicating active choroidal lesions or remain hypofluorescent (type 2) indicating areas of atrophy. There may be presence of numerous hyperfluorescent spots, fuzzy appearance of choroidal vessels in the intermediate phase, and late choroidal hyperfluorescence due to dye leakage which tends to regress after completion of treatment with antitubercular therapy and corticosteroids. The ICGA

Table 9.1 Imaging features of lesions of tubercular serpiginous-like choroiditis

Stage of lesions	FAF features	Features on EDI-OCT	Appearance on ICGA	Features on FA
1	Ill-defined hyper-autofluorescence throughout the lesions	Outer retinal hyper-reflectivity, sub-RPE hyper-reflective deposits, IS-OS disruption, decreased choroidal reflectance	Early and late hypofluorescence; fuzzy margins	Early hypofluorescence with late hyperfluorescence
2	Thin rim of hypo-autofluorescence surrounding the lesion which remains predominantly hyper-autofluorescent	Irregular hyper-reflective elevations in the RPE, IS-OS and ELM disruption, mildly decreased choroidal reflectance	Early hypofluorescence with discrete margins	Early hypofluorescence with late hyperfluorescence
3	Predominantly hypo-autofluorescence of the lesions	Outer retinal hyper-reflective deposits with knob-like elevations of RPE, IS-OS and ELM disruption, atrophy of RPE-Bruch's complex, increased choroidal reflectance	Early hypofluorescence with discrete margins	Early and late hyperfluorescence due to RPE window defects
4	Uniform hypo-autofluorescence of the lesions	Atrophy of outer retinal layers and RPE, IS-OS, and ELM disruption, increased choroidal reflectance, choroidal thinning, loss of choriocapillaris layer	Early and late hypofluorescence	Early and late hyperfluorescence due to RPE window defects

EDI-OCT enhanced-depth imaging optical coherence tomography, *ELM* external limiting membrane, *FA* fluorescein angiography, *ICGA* indocyanine green angiography, *IS-OS* photoreceptor inner segment-outer segment, *OCTA* optical coherence tomography angiography, *RPE* retinal pigment epithelium

changes are usually reversible and may be used to monitor the response to therapy (Figs. 9.1 and 9.2) [22–24].

9.2.3.4 Optical Coherence Tomography

Optical Coherence Tomography Features of Tubercular Serpiginous-Like Choroiditis

OCT features of TB SLC include peripapillary retinal atrophy, disruption of the photoreceptor layer, thinning of retinal pigment epithelium (RPE), mild cystic changes, as well as subretinal fibrosis in the area of old choroidal neovascularization and marked attenuation of the interdigitation zone in the outer retina [25, 26]. In the

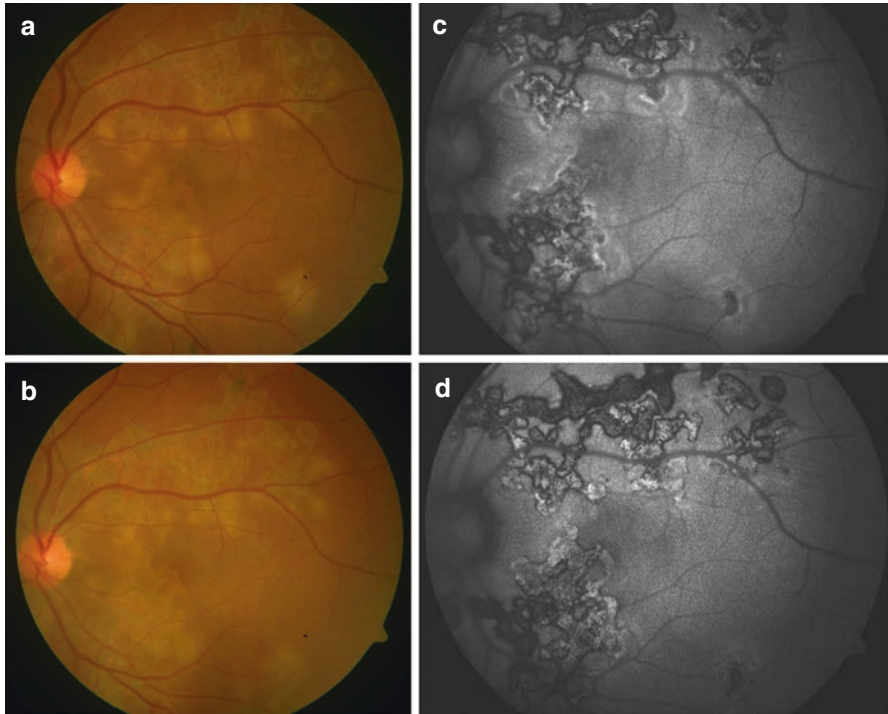


Fig. 9.4 Paradoxical worsening of tubercular serpiginous-like choroiditis (SLC) lesions after initiation of antitubercular therapy (ATT). At presentation, color fundus photography (**a**) shows presence of multifocal choroiditis lesions along the superior vascular arcade and in the inferior macula. Three weeks after initiation of ATT, there is continuous progression of SLC lesions and coalescence in the macula, threatening central vision (**b**). At presentation, fundus autofluorescence (FAF) shows presence of hyper-autofluorescence within the lesion indicating active disease (**c**). Repeat FAF imaging shows increase in the size of the lesions and persistent hyper-autofluorescence (**d**)

acute stage of TB SLC, active edge of the lesions shows a localized, fuzzy area of hyper-reflectivity in the outer retinal layers involving the RPE, photoreceptor outer segment tips, ellipsoid and myoid zones, external limiting membrane, and the outer nuclear layer with no increased backscattering from the inner choroid. As the lesions begin to heal from the center, the hyper-reflective fuzzy areas begin to disappear from OCT scans and are replaced by irregular, hyper-reflective knobby elevations of the outer retinal layers. The RPE, ellipsoid and myoid zones, and the external limiting membrane cannot be distinguished at this stage. There is an increased reflectance from the choroidal layers due to attenuation of the RPE-photoreceptor complex. As the lesions continue to heal further, there is loss of RPE and outer retinal layers and persistent increased reflectance from the choroid on OCT [27].

The technology of enhanced-depth imaging (EDI)-OCT has provided new insights into the choroidal involvement in TB SLC. Using EDI-OCT, choroidal infiltration, elevation of the RPE-Bruch's membrane complex, and focal increase in choroidal thickness have been observed in patients with active TB SLC [27].

Optical Coherence Tomography Features of Tubercular Granulomas

OCT is very useful in the diagnosis and management of tubercular granulomas. Findings on OCT among patients with subretinal granulomas correlate well with ICGA, obviating the need for an invasive procedure. On OCT, an area of localized adhesion between the choriocapillaris-RPE and the overlying neurosensory retina may be observed (*contact sign*) due to inflammatory adhesions overlying the granuloma [28]. Thus, OCT can help to differentiate tubercular choroidal granulomas from other non-inflammatory lesions. In addition, OCT is useful in confirming the presence of exudative retinal detachment associated with choroidal granulomas. On EDI-OCT, active choroidal granulomas generate an increased transmission of the OCT signal toward the sclera. Granulomas in patients affected by TB-related uveitis were more likely to have a lobulated shape and nonhomogeneous internal pattern compared to granulomas related to other entities such as sarcoidosis (Fig. 9.2) [29].

9.2.3.5 Optical Coherence Tomography Angiography

Newer imaging modalities such as optical coherence tomography angiography (OCTA) are being increasingly used in the evaluation of posterior uveitides such as TB-related choroiditis. Using OCTA, choriocapillaris hypoperfusion in association with TB SLC is seen as flow void areas on en face OCTA. These correlate well with findings on ICGA. Thus, noninvasive tools such as OCTA may enable detailed evaluation of the retinochoroidal vasculature among patients with intraocular TB [30]. In a recent report, choroidal neovascularization was detected using OCTA in a patient with tubercular choroiditis [31]. Thus, further advances in imaging may enhance our knowledge of pathogenesis of intraocular TB.

9.2.4 Treatment of Tuberculosis

Treatment of systemic tuberculosis consists of multidrug therapy consisting of first-line antimycobacterial agents such as isoniazid, rifampin, ethambutol, and pyrazinamide, as well as second-line agents such as levofloxacin, streptomycin, and amikacin/kanamycin, among others. The duration and dosing regimen depend on the organ system involved, severity of disease, history of prior anti-TB therapy, and sensitivity of the mycobacteria. In the past decade, there have been increasing cases of multidrug-resistant TB (MDR TB) as well as extensively drug-resistant TB (XDR TB) reported in literature [32–34]. Rifampin resistance has also been recently demonstrated in ocular TB [35].

The treatment of ocular TB consists of four-drug regimen of isoniazid (5 mg/kg/day), rifampicin (10 mg/kg/day), ethambutol (15 mg/kg/day), and pyrazinamide (20–25 mg/kg/day) along with pyridoxine. The clinical features of ocular TB are assessed using retinal and choroidal imaging to assess the activity of the lesions. Ethambutol and pyrazinamide are stopped after a period of 2 months, while isoniazid and rifampin are usually continued for 1 year. Anti-TB therapy is usually given in combination with systemic steroids (oral prednisolone 1 mg/kg/day) which is tapered over the next 6–12 weeks depending upon the level of inflammation. Topical

steroids may be employed in cases with anterior segment inflammation. Systemic immunosuppressants and steroid-sparing agents such as azathioprine may be added as and when required [11]. About 14% patients treated with anti-TB therapy may develop paradoxical worsening of ocular disease (*ocular Jarisch-Herxheimer reaction*) [36]. However, such cases are managed by increasing systemic immunosuppression and not by withholding anti-TB therapy. The role of anti-TB therapy in intraocular TB is to reduce the antigen load by eliminating the bacilli, which may prevent recurrence of the disease.

9.3 Syphilis

Syphilis is a sexually transmitted multisystem disease that is caused by a gram-negative spirochete, *Treponema pallidum*. Syphilis is highly contagious, and the infection can spread through small abrasions on the skin and mucous membranes. In addition, the disease spreads through sexual contact as well as through vertical transmission (transplacental route). The natural history of the acquired disease consists of four stages, namely, primary, secondary, latent, and tertiary syphilis.

9.3.1 Systemic Features of Syphilis

Primary syphilis manifests with a characteristic syphilitic *chancre* that appears as a painless, small ulcer with a hard base in the genital area. Syphilitic chancres are highly contagious and most commonly occur 2–6 weeks after infectious exposure. Although painless, the infective organisms spread from the lesion to involve regional lymph nodes resulting in painless nonsuppurative lymphadenopathy. The chancres usually heal without treatment. However, if left untreated, the organisms spread through the hematogenous route, and the disease often manifests with *secondary syphilis*. During this stage of the disease, the patient may develop fever and maculopapular rash involving the palms and soles. Other common features during this stage include headache, myalgia, and sore throat. Clinical features of secondary syphilis may spontaneously resolve, and the patient may develop *latent syphilis*. Latent syphilis is characterized by disappearance of primary and secondary symptoms though the patient continues to have systemic infection with treponema organisms. Latent syphilis can last for years before the patient develops tertiary disease [37, 38].

Approximately 30–40% patients develop involvement of other organ systems such as the central nervous system and cardiovascular system (*tertiary syphilis*) if left untreated. Tertiary syphilis is characterized by formation of *gumma*. These represent inflammatory infiltrates in the form of a granuloma and appear soft, swollen, rubbery lesions in the skin and other tissues. Tertiary syphilis manifests with *neurosyphilis* [39] that includes cranial nerve palsies, vascular occlusions presenting as strokes or focal neurological deficits, *tabes dorsalis* (syphilitic myelopathy resulting in loss of coordination), and generalized paresis. Patients may also develop

severe dementia and neurological impairment. Cardiovascular involvement presents with aortitis, aortic aneurysms, and valvular insufficiencies. Other organ systems commonly affected include musculoskeletal system, liver, and joints. However, these manifestations have become increasingly rare with antibiotic therapy [38, 40].

With the availability of antibiotics such as penicillin and cephalosporins, the incidence of syphilis dramatically decreased. However, there have been higher numbers of cases reported recently from developed countries like the USA. This may be related to the increasing prevalence of HIV infection [41]. Syphilis coinfection among patients with HIV may result in a highly virulent form of the disease that may rapidly lead to death of the patient.

9.3.2 Ocular Features of Syphilis

Ocular syphilis is most commonly associated with secondary and tertiary syphilis. Ocular involvement occurs in approximately 4–5% of patients with secondary syphilis. The prevalence of syphilis among patients presenting to uveitis referral centers has been estimated to be between 1% and 8% [42].

Pathological manifestations of syphilis can affect any ocular tissue, and the disease can have protean manifestations (Table 9.2). Inflammation can involve the anterior segment, posterior segment, retinal vasculature, optic nerve, and orbit. Therefore, syphilis is referred to as the *great masquerader*. Syphilitic anterior uveitis is typically granulomatous and associated with anterior chamber cells, flare, keratic precipitates, and large iris nodules (Koeppel's or Busacca's nodules). Mild involvement can present with non-granulomatous anterior uveitis. Anterior segment inflammation may be associated with corneal involvement that manifests with interstitial keratitis. Interstitial keratitis is a non-ulcerative corneal stromal condition with sparing of the endothelium and epithelium. This condition presents with inflammation and vascularization with minimal loss of corneal tissue [42–44].

Posterior segment disease most commonly presents with focal or multifocal lesions of chorioretinitis. Lesions of chorioretinitis appear deep yellow-gray with a

Table 9.2 Ocular manifestations of syphilis

Cornea, conjunctiva	Interstitial keratitis, conjunctivitis
Episclera and sclera	Episcleritis, scleritis
Anterior chamber and iris	Anterior uveitis, iritis, iridocyclitis, iris nodules, hypopyon uveitis, iris roseola, gummas of the iris
Posterior segment	Panuveitis, intermediate uveitis, endophthalmitis/panophthalmitis, chorioretinitis, retinal vasculitis, acute syphilitic posterior placoid chorioretinitis, necrotizing retinitis, choroidal detachment, serous retinal detachment, macular edema
Optic nerve and neuro-ophthalmological structures	Optic neuritis, papilledema, neuroretinitis, optic perineuritis, optic atrophy, cranial nerve palsies, visual field defects, Argyll-Robertson pupil, cortical blindness

shallow serous retinal detachment and overlying vitreous inflammation. Severe infection may present with necrotizing retinitis that may mimic acute retinal necrosis [45]. Patients with *necrotizing retinitis* may present with single or multiple yellowish white patches of necrosis often associated with vasculitis, vitreous inflammation, and some anterior segment inflammation [42]. Other manifestations include retinal vasculitis with retinal ischemia. Both retinal veins and arteries may be involved in a focal or diffuse manner. Syphilitic retinal vasculitis may present as *frosted branch angiitis*. *Acute syphilitic posterior placoid chorioretinitis* (ASPPC) is a distinct entity originally described by Gass. Subsequently, a number of cases of ASPPC have been described in literature. The hallmark of ASPPC is presence of a large, placoid lesion in the posterior pole extending beyond the major arcades involving the outer retina and inner choroid (Fig. 9.5). In a series of 16 patients, Eandi et al. [46] have described ASPPC as pale yellowish, ill-defined lesions with a faded center and stippled hyperpigmentation of the RPE that coalesce to become large confluent lesions. These lesions may be associated with vitritis, superficial retinal hemorrhages, retinal vasculitis, disk edema, and serous detachment of the RPE. ASPPC is typically observed among the immunocompromised patients [46].

Syphilitic uveitis can also present with intermediate uveitis and panuveitis. Other ocular features include optic nerve inflammation (*syphilitic optic neuritis*) that may progress to optic atrophy and severe visual field defects. Patients with neurosyphilis may develop pupillary abnormalities (*Argyll-Robertson pupil*) (Table 9.2).

9.3.3 Imaging Features

9.3.3.1 Fundus Photography and Autofluorescence

Chorioretinal lesions of syphilis can be documented using color retinal photography. Color fundus photographs may be used in the follow-up of patients with vitritis, chorioiditis, and other posterior segment diseases to document resolution with therapy. FAF imaging is very useful in the diagnosis of ASPPC. Matsumoto and Spaide have described FAF changes in two patients with FAF. In the area of the placoid lesion, there is usually a slightly increased autofluorescence in a geographic pattern. In addition, focal intensely hyper-autofluorescent spots may also be found [47]. Other features on FAF include punctate hypo-autofluorescent spots (Fig. 9.5) [46].

9.3.3.2 Fluorescein Angiography

FA provides useful information regarding the pathology of syphilitic posterior uveitis. On FA, lesions of chorioretinitis show early hypofluorescence followed by late staining. Lesions of ASPPC show early central hypofluorescence or faint hyperfluorescence followed by progressive hyperfluorescence in the area of the lesion. Variable or punctate hypofluorescence producing a classic *leopard spot* pattern may be seen in later stages of the disease. FA may also be useful in the detection of macular edema and optic nerve head inflammation among patients with syphilitic uveitis [46].

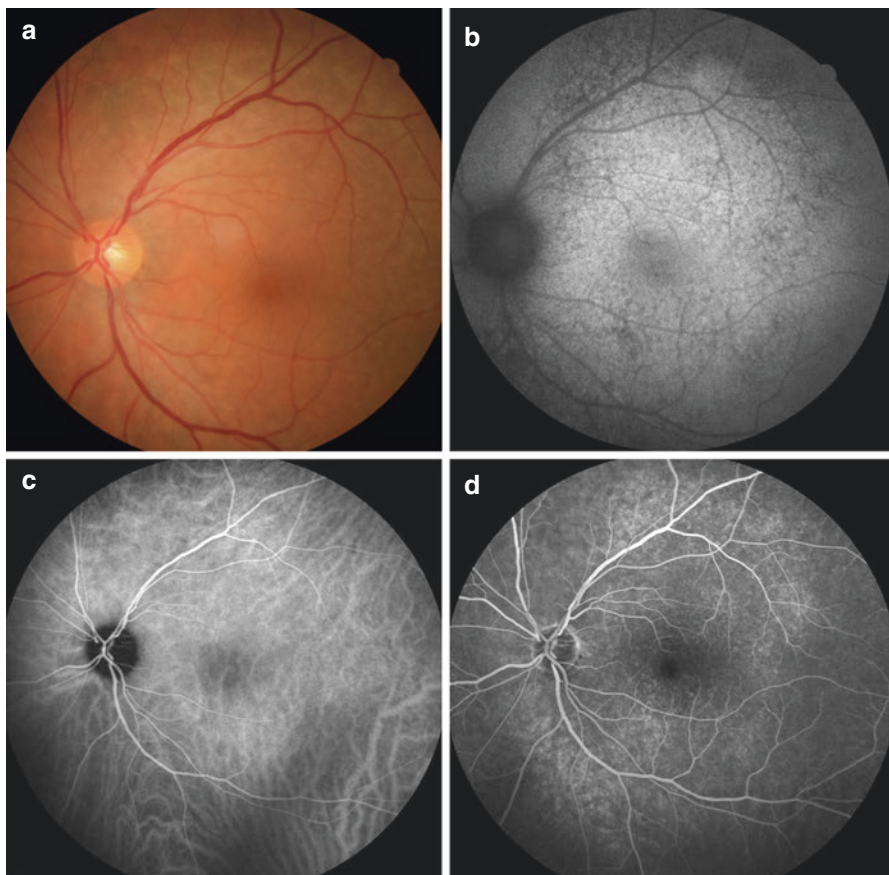


Fig. 9.5 Multimodal imaging of a patient with acute syphilitic posterior placoid chorioretinitis (ASPPC). Color fundus photography shows presence of a large, diffuse, placoid lesion involving the posterior pole and extending to the mid-periphery (a). Fundus autofluorescence shows presence of diffuse hyper-autofluorescence of the lesion with scattered focal areas of hypo-autofluorescence (b). Indocyanine green angiography (c) shows subtle hypofluorescence along the lesion. Fluorescein angiography (d) in the late phase shows punctate hyperfluorescence without any leakage. (Image courtesy: Dr. Alessandro Invernizzi, MD, University of Milan, Italy)

9.3.3.3 Indocyanine Green Angiography

Characteristic features of ICGA among patients with ASPPC have been described in various reports. Lesions of ASPPC show variable hypofluorescence in both early and late stages on ICGA. In some patients, there may be late hyperfluorescence on ICGA [42, 46]. ICGA is a useful tool to demonstrate choroidal vascular involvement among patients with syphilitic posterior uveitis (Fig. 9.5).

9.3.3.4 Optical Coherence Tomography

Serial imaging using OCT is very useful in the diagnosis and follow-up of patients with posterior segment manifestations associated with syphilis. Recent studies by Brito et al. and Pichi et al. have described the OCT features of ASPPC [48, 49]. During the early stage of the disease (within 1–2 days of presentation), OCT may show presence of a small amount of subretinal fluid, an intact external limiting membrane, disruption of the ellipsoid and myoid zone, and thickening and *granular hyper-reflectivity of the RPE* (without nodular elevations) (Fig. 9.6). Subsequently (7–10 days after presentation), subretinal fluid may resolve on OCT, but the scans may show an irregular thickening and hyper-reflectivity of the RPE with *prominent nodular elevations*, along with a loss of ellipsoid and myoid zones, and RPE bands. In addition, there may be areas of punctate hyper-reflectivity in the choroid.

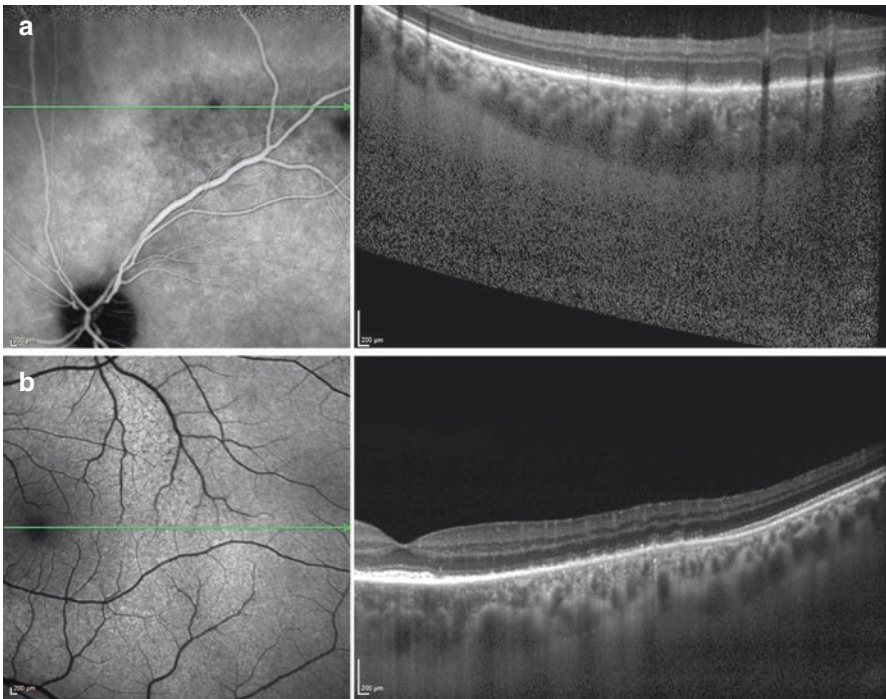


Fig. 9.6 Enhanced-depth imaging (EDI) optical coherence tomography (OCT) of a patient with acute syphilitic posterior placoid chorioretinitis (ASPPC). Combined indocyanine *green* angiography (ICGA) and EDI-OCT (a) show hypofluorescence on ICGA, and corresponding OCT B-scan shows granular hyper-reflectivity of the retinal pigment epithelium (RPE). There is mild choroidal thickening. Combined fundus autofluorescence and EDI-OCT B-scan passing through the macula in the same patient show macular RPE thickening and focal hyper-reflectivity in the region temporal to the fovea (b). (Image courtesy: Dr. Alessandro Invernizzi, MD, University of Milan, Italy)

Macular OCT may be useful in the detection of macular edema associated with syphilitic uveitis. OCT may also demonstrate presence of subretinal fluid along with outer retinal disruption. Retinal nerve fiber layer edema can be detected among patients with optic nerve head swelling using OCT.

9.3.3.5 Advanced Imaging Modalities

Newer imaging modalities such as the swept-source OCT may provide significant insights into the disease pathophysiology especially among cases presenting with ASPPC. Using swept-source OCT, superior imaging of the outer retina and inner choroid may be possible, leading to improved understanding of the nodular elevations and other changes observed on spectral-domain OCT. EDI-OCT imaging along with tools such as OCTA may provide information on inner choroidal changes among patients with syphilis.

9.3.4 Treatment of Ocular and Systemic Syphilis

Penicillin G is considered to be the preferred drug for the treatment of all stages of syphilis. Based on the stage of syphilis, preparation, dosage, and length of treatment may vary. Penicillin G is available in benzathine, aqueous, procaine, and crystalline preparations. Treatment of secondary and tertiary syphilis is typically longer compared to primary syphilis. Ocular syphilis is treated similar to neurosyphilis since these sites have relatively impermeable blood barriers. Aqueous penicillin G (18–24 million units/day intravenous for 10–14 days) or procaine penicillin G (2.4 million units intramuscular once a day for 10–14 days) in combination with probenecid (500 mg four times a day orally) is preferred for ocular syphilis. Alternatively, ceftriaxone (2 g/day intravenous for 10–14 days) can be employed for patients with penicillin allergy [50]. Topical steroids can be used for anterior segment inflammation and keratitis. Systemic steroids may be used adjunctively for posterior uveitis with significant intraocular inflammation and vitritis [45].

9.4 Lyme Disease

Lyme disease is a multisystem infectious disease caused by a spirochete, *Borrelia burgdorferi*, and transmitted by the ticks of *Ixodes ricinus* complex [51]. This condition is endemic in more than 20 states in the USA as well as in Europe and parts of Asia [52]. In the USA, more than 93% cases have been reported from *Northeastern states* such as Connecticut, Delaware, and Massachusetts [53]. The incidence of Lyme disease is highest among boys in the age range of 5–9 years and persons of both sexes in the age range of 60–64 years with an overall annual incidence of 106.6/100,000 persons in the USA [54]. A number of studies from European countries such as Italy, Bulgaria, and Belgium have also shown a variable incidence rate

based on the local vector population [55–57]. A number of cases have been reported from India and China highlighting the need for continuous surveillance in non-endemic areas as well [58, 59].

9.4.1 Systemic Features of Lyme Disease

Lyme disease consists of three clinical stages: early infection with localized erythema migrans (stage 1); systemic dissemination that presents with cardiac, neurological, and articular involvement (stage 2); and late or persistent infection (stage 3) [60–62]. Early signs and symptoms may develop within 3–30 days after a tick bite. Common features include fever, chills, headache, and fatigue. *Erythema migrans* (EM) is a typical rash that occurs at the site of the tick bite. EM occurs in 70–80% individuals and can reach a size of 12 inches or more. EM has a bull’s eye appearance with partial central clearing and a bright red border. Systemic dissemination may present months after a tick bite. Common clinical features include neurological involvement which presents with headache and neck stiffness. Patients may present with *bilateral facial palsy*, ataxia, and myelitis. *Lyme carditis* may present with myocarditis or atrioventricular block. There may be severe, disabling arthritis or persistent chronic articular inflammation [52]. Patients with Lyme disease may also develop posttreatment Lyme disease syndrome (*chronic Lyme disease*), an obscure entity that presents with fatigue, pain, and joint or muscle ache [63].

9.4.2 Ocular Features of Lyme Disease

Ocular features of Lyme disease can occur during the early stage or in the late stage, several months to years after primary infection [64]. Conjunctivitis is the most common manifestation of Lyme disease and presents during the early stage of the disease. It may be associated with periorbital edema. Neuro-ophthalmic manifestations also occur early during the course of the infection [65]. Other ocular features during stage 2 (stage of systemic dissemination) include blepharospasm, endophthalmitis/panophthalmitis, cystoid macular edema, optic neuritis (Fig. 9.7), retinal vasculitis, Horner’s syndrome, and Argyll-Robertson pupil. Conditions such as stromal/nummular keratitis, episcleritis, and orbital myositis occur during stage 3 of the disease (Table 9.3) [65–68].

Intermediate uveitis or posterior uveitis in Lyme disease may be accompanied by retinal vasculitis. Patients with Lyme disease may also present with lesions of multifocal choroiditis that appear as small, round, and punched-out along with variable vitreous inflammation [69]. Other posterior segment findings in Lyme disease include acute exudative polymorphous vitelliform maculopathy (AEPVM) [70], neuroretinitis, and inflammatory choroidal neovascularization. Orbital myositis may present with thickening of extraocular muscles, lid edema, proptosis, ptosis, or dacryoadenitis.

Fig. 9.7 Fluorescein angiography (FA) of a patient with Lyme disease-related optic neuritis, retinal vasculitis, and macular edema. Ultrawide-field FA (a) shows disk hyperfluorescence in the late phase, cystoid macular edema, and peripheral focal vascular leakage (predominantly venular). Magnified view (b) shows presence of optic neuritis and macular edema

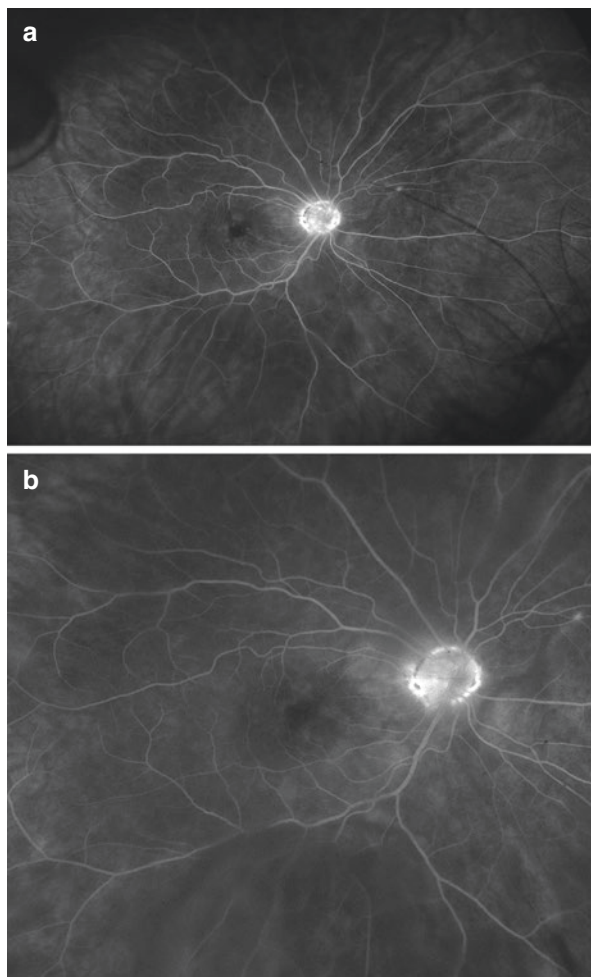


Table 9.3 Ocular features of Lyme disease

Stage of the disease	Ocular features
1	Conjunctivitis, periorbital edema
2	Blepharospasm, uveitis (iridocyclitis/iritis), panophthalmitis, choroiditis, optic disk edema, macular edema, optic neuritis, pseudotumor cerebri, ischemic optic neuropathy, optic atrophy, Horner's syndrome, Argyll-Robertson pupil
3	Corneal involvement (stromal/nummular keratitis), episcleritis, orbital myositis, cortical blindness

9.4.3 Imaging Features

9.4.3.1 Fundus Photography

Among patients with Lyme disease, clinical fundus photography may be useful to document presence of vitreous haze. Choroidal lesions of Lyme disease appear as focal, punched-out lesions mostly involving the posterior pole and mid-periphery. There may be associated inflammatory choroidal neovascularization. Lesions of AEPVM present with multifocal serous retinal detachment and accumulation of deposits in the outer retinal layer [70].

9.4.3.2 Fluorescein Angiography

The appearance of chorioretinal lesions in Lyme disease on FA is similar to lesions of syphilis. Chorioretinal lesions demonstrate early hypofluorescence followed by late staining. Among patients with Lyme disease, FA may be useful to detect the presence of retinal vascular leakage due to vasculitis. Retinal vasculitis may be rarely associated with occlusion and ischemia. Optic nerve head hyperfluorescence suggests presence of optic neuritis (Fig. 9.7) [71, 72].

9.4.3.3 Optical Coherence Tomography

OCT imaging may help in characterizing the chorioretinal involvement in Lyme disease. OCT is useful in demonstrating swelling of the optic nerve head among patients with optic neuritis. Significant number of patients with Lyme disease may have cystoid macular edema that can be diagnosed and followed using OCT [67, 68].

9.4.4 Treatment of Lyme Disease

The treatment of Lyme disease consists of systemically administered antibiotics such as beta-lactams and tetracyclines along with corticosteroids [73]. Early Lyme disease that manifests with erythema migrans can be treated with oral doxycycline (100 mg twice a day), amoxicillin (500 mg three times a day), or cefuroxime axetil (500 mg twice a day) for 2 weeks. Macrolide antibiotics and first-generation cephalosporins such as cephalexin are not recommended for early Lyme disease. Drugs used in children include doxycycline (4–8 mg/kg/day) or amoxicillin (50 mg/kg/day) [73].

Intravenous route of administration may be employed for patients with neurological manifestations and advanced disease affecting the cardiovascular system. The treatment regimen consists of ceftriaxone or cefotaxime 2 g/day for 2–4 weeks [73–75]. There are no guidelines available in literature that guide therapy for ocular Lyme disease. Treatment of ocular disease depends on disappearance of serum antibody titers. Concomitant systemic or topical corticosteroids can be used to treat associated inflammation.

9.5 Cat Scratch Disease

Cat scratch disease (CSD) is also known as bartonellosis. CSD is a zoonotic infection caused by a gram-negative bacillus, *Bartonella henselae*. Domestic cats serve as the primary mammalian reservoir of this organism. *Ctenocephalides felis* (cat flea) is the arthropod vector that spreads the disease. Human infection is usually caused by scratch from an infected cat or contamination of surface wounds [76, 77]. The worldwide seroprevalence of this condition is estimated to be approximately 20%. Annual incidence of CSD based on national outpatient database in the USA is estimated to be 9.3/100,000 [78]. A pooled analysis of a large number of CSD cases was performed in Turkey [79]. In a small study conducted in Italy, 21% patients awaiting heart transplant were diagnosed to be seropositive for *B. henselae* [80].

9.5.1 Systemic Features of Cat Scratch Disease

CSD is commonly seen in children and young adults. The condition starts with a vesicular eruption at the site of inoculation. Following dissemination of the organism, tender regional lymphadenopathy develops within 1–2 weeks. Other systemic features include malaise, fever, anorexia, and arthralgia. Visceral involvement may present with hepatosplenomegaly. Rarely, CSD may present with meningoencephalitis, seizures, headache, and other neurological complaints. Cardiac involvement may present with endocarditis. Among immunocompromised subjects, CSD may present with a characteristic systemic features such as *bacillary angiomatosis* and *peliosis*. Bacillary angiomatoses are vascular proliferative lesions that appear red/purple papules on the skin and mucous membranes. These resemble vascular lesions of Kaposi's sarcoma [81, 82]. *Peliosis hepatitis* is an uncommon presentation with abdominal pain, nausea, and vomiting due to vascular lesions in the liver [83, 84].

9.5.2 Ocular Features of Cat Scratch Disease

Ocular manifestations of CSD can be divided into two categories: primary involvement (*Parinaud oculoglandular syndrome*) or secondary involvement due to systemic dissemination of the disease. Parinaud oculoglandular syndrome manifests with conjunctivitis, conjunctival granulomas, stromal keratitis, and orbital inflammation. Neuro-ophthalmic manifestations include optic nerve head edema, *neuroretinitis* [85], and inflammatory mass lesions involving the optic nerve. Retinochoroidal inflammation may manifest as juxtapapillary chorioretinitis that appear as cotton-wool spots. There may be accompanying satellite lesions in the retina. Vascular abnormalities such as angiomatous-like proliferation (similar to bacillary angiomatosis) (Fig. 9.8), branch retinal arteriole occlusion, or retinal vasculitis may be seen on careful examination. Other ocular features of CSD include serous retinal detachment, panuveitis, and intermediate uveitis [86, 87].

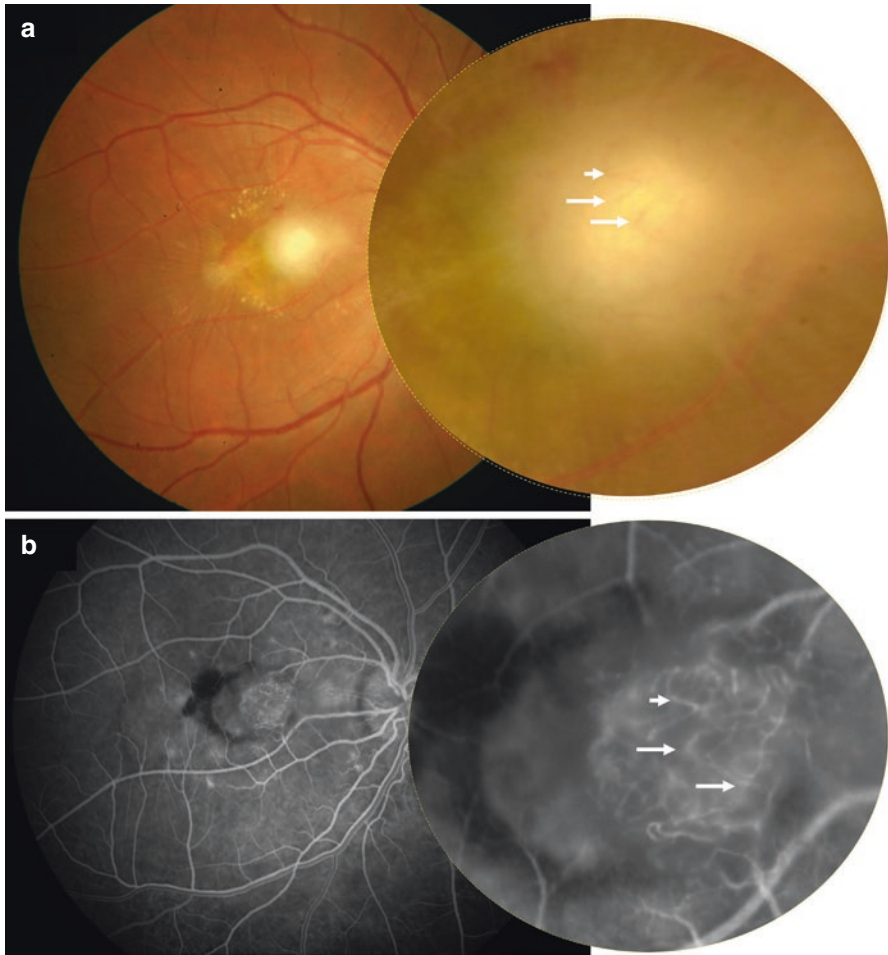


Fig. 9.8 Fundus photography and fluorescein angiography (FA) of a patient with cat scratch disease. A *yellowish-white* lesion with fuzzy edges, surrounding exudation, subretinal fluid, and internal limiting membrane wrinkling is seen on color fundus photography (**a**). Magnified view shows characteristic vascular pattern within the lesion. FA (early transit phase) (**b**) shows hyperfluorescence of the lesion with surrounding focal areas of hyperfluorescence (satellite lesions). Magnified view shows characteristic pattern of vascular proliferation reminiscent of bacillary angiomatosis

9.5.3 Imaging Features

9.5.3.1 Fundus Photography and Autofluorescence

Chorioretinal lesions of CSD can be documented using color fundus photography. Neuroretinitis presents with optic nerve head edema with a macular star formation due to exudation. In addition, internal limiting membrane wrinkling may be observed. Lesions of retinitis may appear dark on FAF because of blockade of the normal RPE autofluorescence due to the overlying retinitis lesion.

9.5.3.2 Fluorescein and Indocyanine Green Angiography

Lesions of CSD present with abnormal dye leakage on FA. In the early phase, juxtapapillary granulomas of CSD may present with dye leakage on FA. Abnormal retinal vascular patterns reminiscent of bacillary angiomatosis may be observed on FA [88]. Occasionally, chorioretinal lesions may present with only late leakage [89]. Other features seen on FA include cystoid macular edema, retinal vasculitis, and satellite lesions (Figs. 9.8 and 9.9). Atypical presentations of CSD on FA include retinal non-perfusion due to occlusive vasculitis [90]. Optic neuritis manifests as optic disk hyperfluorescence, which may be rarely associated with optic nerve neovascularization [91]. Serous retinal detachment may result in extensive pooling of the dye in the posterior pole or in the peripapillary region.

ICGA features of CSD include diffuse choroidal leakage and hypofluorescence in the region corresponding to the subretinal granulomas. However, the leakage observed on ICGA is typically lesser in amount compared to FA [88]. In addition, patients with optic neuritis may show hyperfluorescence of the optic nerve head on ICGA.

9.5.3.3 Optical Coherence Tomography

OCT is a useful imaging modality in the management of patients with CSD that helps in the characterization of retinitis lesions and detection of subretinal/choroidal neovascularization [92]. Serous retinal detachment or intraretinal fluid accumulation leading to macular edema can be seen on macular OCT. [93] Chorioretinal lesions of CSD appear as hyper-reflective deposits in the inner retinal layers with shadowing on the posterior retinal layers and the choroid (Fig. 9.10). Such changes are known to progressively diminish with antibiotic therapy [94].

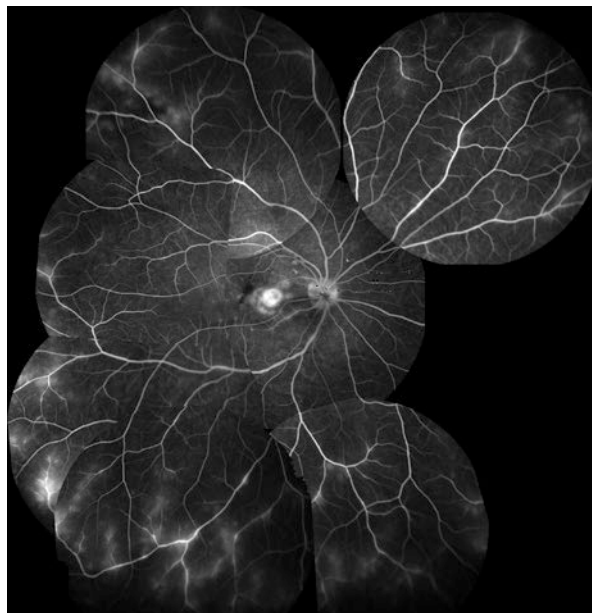


Fig. 9.9 Montage view of fluorescein angiography of a patient with cat scratch disease shows presence of significant peripheral vascular leakage suggestive of active vasculitis

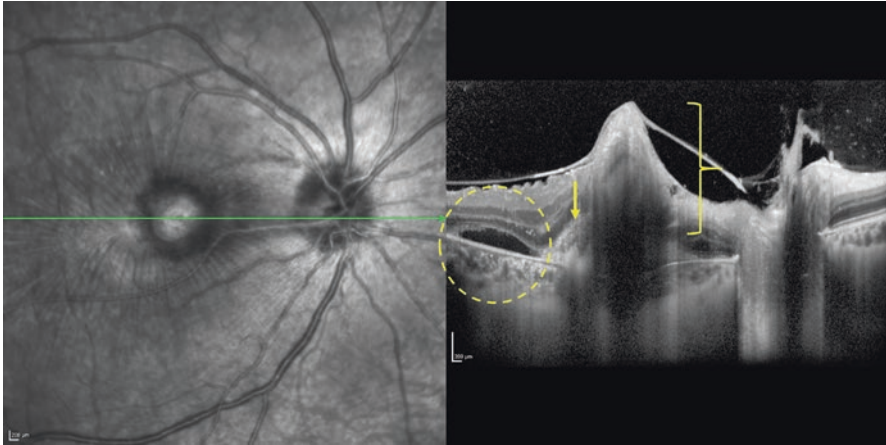


Fig. 9.10 Enhanced-depth imaging optical coherence tomography (EDI-OCT) of a patient with cat scratch disease shows presence of vitreous inflammation, full-thickness retinal involvement (*square bracket*), subretinal hyper-reflective material suggestive of choroidal neovascularization (*yellow arrow*), and subretinal fluid (*dashed circle*)

9.5.4 Treatment of Cat Scratch Disease

Treatment of CSD consists of systemic antibiotics. Concomitant corticosteroids (topical or oral prednisone) may be used for ocular CSD in the presence of severe inflammatory reaction. Antibiotics commonly employed in CSD include azithromycin, trimethoprim-sulfamethoxazole, ciprofloxacin, gentamicin, and rifampin [95]. Recommended therapy consists of azithromycin for patients with moderate to severe disease. For immunocompetent patients with mild to moderate disease, no antibiotic treatment may have a higher benefit-to-risk ratio. Among patients with severe disease, or immunocompromised status, combination of intravenous or oral doxycycline (100 mg twice daily) and rifampin (300 mg twice daily) may be used [96]. However, a recent report suggests that antibiotic therapy may not significantly affect the cure rate or the time to achieve cure among patients with CSD [95].

9.6 Future Directions

In the past decade, a number of advances have been made in the field of retinal and choroidal imaging. There has been an increasing trend toward the development of noninvasive and ultrahigh-speed imaging tools that can provide novel information about various uveitic entities. Systemic infections such as tuberculosis and syphilis commonly involve the choroid, which is often difficult to image using conventional modalities. Thus far, ICGA was the only tool to assess involvement of choroid and deeper structures. However, introduction of EDI-OCT, and more recently the swept-source OCT, is likely to greatly supplement conventional dye-based techniques such

as ICGA in the evaluation of such clinical entities. The novel technology of OCTA also appears to be very useful in the management of intraocular tuberculosis. With the help of next-generation imaging technologies and availability of advanced image analysis software in the future, it is hoped that fast, noninvasive office procedures would provide detailed information regarding the pathology of ocular involvement in systemic infections.

Key Learning Points

- Systemic infectious diseases such as tuberculosis, syphilis, and cat scratch disease can have protean ophthalmic features that may lead to diagnostic challenges.
- Ancillary imaging tools such as fluorescein angiography, indocyanine green angiography, and optical coherence tomography, among others, are indispensable tools in the complete evaluation of patients with uveitis in order to establish accurate diagnosis and assess severity of the disease.
- Serial imaging using these techniques may enable precise assessment of response to therapy. This can be achieved noninvasively using modern techniques such as optical coherence tomography.
- With the development of advanced imaging technology such as swept-source optical coherence tomography and optical coherence tomography angiography, newer insights into the pathophysiology of diseases such as tuberculosis have been highlighted in literature.
- Further research in the field of retinal and choroidal imaging is likely to improve our understanding of the natural history of systemic infectious diseases that affect various ocular structures.

Financial Support The authors have no financial disclosure/proprietary interest. No conflicting relationship exists for any author.

This work was partly supported by a grant from the Department of Science and Technology, India, for the development of Centre of Excellence at the Advanced Eye Centre, PGIMER, Chandigarh.

References

1. Singh R, Gupta V, Gupta A. Pattern of uveitis in a referral eye clinic in north India. *Indian J Ophthalmol.* 2004;52(2):121–5.
2. Gupta A, Gupta V. Tubercular posterior uveitis. *Int Ophthalmol Clin.* 2005;45(2):71–88.
3. Hooper C, McCluskey P. Intraocular inflammation: its causes and investigations. *Curr Allergy Asthma Rep.* 2008;8(4):331–8.
4. WHO. Guidelines on the management of latent tuberculosis infection. Geneva: World Health Organization; 2015.
5. Global Health Observatory (GHO) data. 2014. <http://www.who.int/gho/tb/en/>. Accessed 27 Apr 2016.
6. Behr MA, Waters WR. Is tuberculosis a lymphatic disease with a pulmonary portal? *Lancet.* 2014;14(3):250–5.

7. Narendran G, Swaminathan S. TB-HIV co-infection: a catastrophic comradeship. *Oral Dis.* 2016;22(Suppl 1):46–52.
8. Balasubramanian V, Wiegand EH, Taylor BT, Smith DW. Pathogenesis of tuberculosis: pathway to apical localization. *Tuber Lung Dis.* Jun 1994;75(3):168–78.
9. Lara LP, Ocampo V Jr. Prevalence of presumed ocular tuberculosis among pulmonary tuberculosis patients in a tertiary hospital in the Philippines. *J Ophthalm Inflamm Infect.* 2013; 3(1):1.
10. Gupta V, Shouhgy SS, Mahajan S, et al. Clinics of ocular tuberculosis. *Ocul Immunol Inflamm.* 2015;23(1):14–24.
11. Gupta V, Gupta A, Rao NA. Intraocular tuberculosis—an update. *Surv Ophthalmol.* 2007;52(6):561–87.
12. Gupta A, Bansal R, Gupta V, Sharma A, Bambery P. Ocular signs predictive of tubercular uveitis. *Am J Ophthalmol.* 2010;149(4):562–70.
13. Bansal R, Gupta A, Gupta V, Dogra MR, Sharma A, Bambery P. Tubercular serpiginous-like choroiditis presenting as multifocal serpiginoid choroiditis. *Ophthalmology.* 2012;119(11):2334–42.
14. Gupta V, Gupta A, Arora S, Bambery P, Dogra MR, Agarwal A. Presumed tubercular serpiginouslike choroiditis: clinical presentations and management. *Ophthalmology.* 2003;110(9):1744–9.
15. Nazari Khanamiri H, Rao NA. Serpiginous choroiditis and infectious multifocal serpiginoid choroiditis. *Surv Ophthalmol.* 2013;58(3):203–32.
16. Zhang M, Zhang J, Liu Y. Clinical presentations and therapeutic effect of presumed choroidal tuberculosis. *Retina.* 2012;32(4):805–13.
17. Biswas J, Madhavan HN, Gopal L, Badrinath SS. Intraocular tuberculosis. Clinicopathologic study of five cases. *Retina.* 1995;15(6):461–8.
18. Babu RB, Sudharshan S, Kumarasamy N, Therese L, Biswas J. Ocular tuberculosis in acquired immunodeficiency syndrome. *Am J Ophthalmol.* 2006;142(3):413–8.
19. Sudharshan S, Kaleemunnisha S, Banu AA, et al. Ocular lesions in 1,000 consecutive HIV-positive patients in India: a long-term study. *J Ophthalm Inflamm Infect.* 2013;3(1):2.
20. Gupta A, Bansal R, Gupta V, Sharma A. Fundus autofluorescence in serpiginouslike choroiditis. *Retina.* 2012;32(4):814–25.
21. Aggarwal K, Mulkutkar S, Mahajan S, et al. Role of ultra-wide field imaging in the management of tubercular posterior uveitis. *Ocul Immunol Inflamm.* 2016;6:1–6.
22. Wolfensberger TJ, Piguet B, Herbort CP. Indocyanine green angiographic features in tuberculous chorioretinitis. *Am J Ophthalmol.* 1999;127(3):350–3.
23. De Luigi G, Mantovani A, Papadia M, Herbort CP. Tuberculosis-related choriocapillaritis (multifocal-serpiginous choroiditis): follow-up and precise monitoring of therapy by indocyanine green angiography. *Int Ophthalmol.* 2012;32(1):55–60.
24. Invernizzi A, Agarwal A, Cozzi M, Viola F, Nguyen QD, Staurengi G. Enhanced depth imaging optical coherence tomography features in areas of choriocapillaris hypoperfusion. *Retina.* 2016;36(10):2013–21.
25. Punjabi OS, Rich R, Davis JL, et al. Imaging serpiginous choroidopathy with spectral domain optical coherence tomography. *Ophthalmic Surg Lasers Imaging.* 2008;39(4 Suppl):S95–8.
26. Rifkin LM, Munk MR, Baddar D, Goldstein DA. A new OCT finding in tubercular serpiginous-like choroidopathy. *Ocul Immunol Inflamm.* 2015;23(1):53–8.
27. Bansal R, Kulkarni P, Gupta A, Gupta V, Dogra MR. High-resolution spectral domain optical coherence tomography and fundus autofluorescence correlation in tubercular serpiginouslike choroiditis. *J Ophthalm Inflamm Infect.* 2011;1(4):157–63.
28. Salman A, Parmar P, Rajamohan M, Vanila CG, Thomas PA, Jesudasan CA. Optical coherence tomography in choroidal tuberculosis. *Am J Ophthalmol.* 2006;142(1):170–2.
29. Invernizzi A, Mapelli C, Viola F, et al. Choroidal granulomas visualized by enhanced depth imaging optical coherence tomography. *Retina.* 2015;35(3):525–31.
30. Mandadi SK, Agarwal A, Aggarwal K, Moharana B, Singh R, Sharma A, Bansal R, Dogra MR, Gupta V. For OCTA Study Group. Novel findings on optical coherence tomography

- angiography in patients with tubercular serpiginous-like choroiditis. *Retina*. 2016 Dec 7. [Epub ahead of print].
31. Yee HYM, Keane PAF, Ho SLF, Agrawal RF. Optical coherence tomography angiography of choroidal neovascularization associated with tuberculous serpiginous-like choroiditis. *Ocular Immunol Inflamm*. 2016;30:1–3.
 32. Marks SM, Hirsch-Moverman Y, Salcedo K, et al. Characteristics and costs of multidrug-resistant tuberculosis in-patient care in the United States, 2005–2007. *IntJ Tuber Lung Dis*. 2016;20(4):435–41.
 33. Tiberi S, Sotgiu G, D’Ambrosio L, et al. Comparison of effectiveness and safety of imipenem/clavulanate- versus meropenem/clavulanate-containing regimens in the treatment of MDR- and XDR-TB. *Eur Respir J*. 2016;47(6):1758–66.
 34. Sotgiu G, D’Ambrosio L, Centis R, et al. Carbapenems to treat multidrug and extensively drug-resistant tuberculosis: a systematic review. *Int J Mol Sci*. 2016;17(3):373.
 35. Sharma K, Sharma A, Bansal R, Fiorella PD, Gupta A. Drug-Resistant Tubercular Uveitis. *J Clin Microbiol*. Nov 2014;52(11):4113–4.
 36. Gupta V, Bansal R, Gupta A. Continuous progression of tubercular serpiginous-like choroiditis after initiating antituberculosis treatment. *Am J Ophthalmol*. 2011;152(5):857–863.e852.
 37. Eickhoff CA, Decker CF. Syphilis. *Dis Mon*. 2016;62:280–6.
 38. Mitja O, Asiedu K, Mabey D. Yaws. *Lancet*. 2013;381(9868):763–73.
 39. Berger JR, Dean D. Neurosyphilis. *Handb Clin Neurol*. 2014;121:1461–72.
 40. Lynn WA, Lightman S. Syphilis and HIV: a dangerous combination. *Lancet*. 2004;4(7):456–66.
 41. Centers for Disease Control and Prevention (CDC). Outbreak of syphilis among men who have sex with men--Southern California, 2000. *MMWR Morb Mortal Wkly Rep*. 2001;50(7):117–20.
 42. Davis JL. Ocular syphilis. *Curr Opin Ophthalmol*. 2014;25(6):513–8.
 43. Yang P, Zhang N, Li F, Chen Y, Kijlstra A. Ocular manifestations of syphilitic uveitis in Chinese patients. *Retina*. 2012;32(9):1906–14.
 44. Doris JP, Saha K, Jones NP, Sukthankar A. Ocular syphilis: the new epidemic. *Eye*. 2006;20(6):703–5.
 45. Chao JR, Khurana RN, Fawzi AA, Reddy HS, Rao NA. Syphilis: reemergence of an old adversary. *Ophthalmology*. 2006;113(11):2074–9.
 46. Eandi CM, Neri P, Adelman RA, Yannuzzi LA, Cunningham ET Jr. Acute syphilitic posterior placoid chorioretinitis: report of a case series and comprehensive review of the literature. *Retina*. 2012;32(9):1915–41.
 47. Matsumoto Y, Spaide RF. Autofluorescence imaging of acute syphilitic posterior placoid chorioretinitis. *Retinal Cases Brief Rep*. 2007;1(3):123–7.
 48. Brito P, Penas S, Carneiro A, Palmares J, Reis FF. Spectral-domain optical coherence tomography features of acute syphilitic posterior placoid chorioretinitis: the role of autoimmune response in pathogenesis. *Case Rep Ophthalmol*. 2011;2(1):39–44.
 49. Pichi F, Ciardella AP, Cunningham ET Jr, et al. Spectral domain optical coherence tomography findings in patients with acute syphilitic posterior placoid chorioretinopathy. *Retina*. 2014;34(2):373–84.
 50. Clement ME, Okeke NL, Hicks CB. Treatment of syphilis: a systematic review. *JAMA*. 2014;312(18):1905–17.
 51. Lane RS, Piesman J, Burgdorfer W. Lyme borreliosis: relation of its causative agent to its vectors and hosts in North America and Europe. *Annu Rev. Entomol*. 1991;36:587–609.
 52. Steere AC. Lyme disease. *N Engl J Med*. 2001;345(2):115–25.
 53. Bacon RM, Kugeler KJ, Mead PS. Surveillance for Lyme disease--United States, 1992–2006. *Morb Mortal Wkly Rep*. 2008;57(10):1–9.
 54. Nelson CA, Saha S, Kugeler KJ, et al. Incidence of clinician-diagnosed lyme disease, United States, 2005–2010. *Emerg Infect Dis*. 2015;21(9):1625–31.
 55. Cimmino MA, Fumarola D, Sambri V, Accardo S. The epidemiology of Lyme borreliosis in Italy. *Microbiologica*. 1992;15(4):419–24.

56. Christova I, Komitova R. Clinical and epidemiological features of Lyme borreliosis in Bulgaria. *Wien Klin Wochenschr.* 2004;116(1–2):42–6.
57. Bleyenheuft C, Lernout T, Berger N, et al. Epidemiological situation of Lyme borreliosis in Belgium, 2003 to 2012. *Arch Public Health.* 2015;73(1):33.
58. Dou XF, Lyu YN, Jiang Y, et al. Lyme borreliosis-associated risk factors in residents of Beijing suburbs: a preliminary case-control study. *Biomed Environ Sci.* 2014;27(10):807–10.
59. Jairath V, Sehrawat M, Jindal N, Jain VK, Aggarwal P. Lyme disease in Haryana, India. *Ind J Dermatol Venereol Leprol.* 2014;80(4):320–3.
60. Sanchez JL. Clinical manifestations and treatment of lyme disease. *Clin Lab Med.* 2015;35(4):765–78.
61. Hoppa E, Bachur R. Lyme disease update. *Curr Opin Pediatr.* 2007;19(3):275–80.
62. Chomel B. Lyme disease. *Rev Sci Tech.* 2015;34(2):569–76.
63. Halperin JJ. Chronic Lyme disease: misconceptions and challenges for patient management. *Infect Drug Resist.* 2015;8:119–28.
64. Raja H, Starr MR, Bakri SJ. Ocular manifestations of tick-borne diseases. *Surv Ophthalmol.* 2016;61(6):726–44.
65. Winterkorn JM. Lyme disease: neurologic and ophthalmic manifestations. *Surv Ophthalmol.* 1990;35(3):191–204.
66. Balcer LJ, Winterkorn JM, Galetta SL. Neuro-ophthalmic manifestations of Lyme disease. *J Neuroophthalmol.* 1997;17(2):108–21.
67. Bergloff J, Gasser R, Feigl B. Ophthalmic manifestations in Lyme borreliosis. A review. *J Neuroophthalmol.* 1994;14(1):15–20.
68. Park M. Ocular manifestations of Lyme disease. *J Am Optom Assoc.* 1989;60(4):284–9.
69. Lardenoye CW, Van der Lelij A, de Loos WS, Treffers WF, Rothova A. Peripheral multifocal chorioretinitis: a distinct clinical entity? *Ophthalmology.* 1997;104(11):1820–6.
70. Singh RS, Tran LH, Kim JE. Acute exudative polymorphous vitelliform maculopathy in a patient with Lyme disease. *Ophthalm Surg Lasers Imag Retina.* 2013;44(5):493–6.
71. Karma A, Mikkila H. Ocular manifestations and treatment of Lyme disease. *Curr Opin Ophthalmol.* 1996;7(3):7–12.
72. Karma A, Seppala I, Mikkila H, Kaakkola S, Viljanen M, Tarkkanen A. Diagnosis and clinical characteristics of ocular Lyme borreliosis. *Am J Ophthalmol.* 1995;119(2):127–35.
73. Wormser GP, Dattwyler RJ, Shapiro ED, et al. The clinical assessment, treatment, and prevention of lyme disease, human granulocytic anaplasmosis, and babesiosis: clinical practice guidelines by the Infectious Diseases Society of America. *Clin Infect Dis.* 2006;43(9):1089–134.
74. Wright WF, Riedel DJ, Talwani R, Gilliam BL. Diagnosis and management of Lyme disease. *Am Fam Physician.* 2012;85(11):1086–93.
75. Bratton RL, Whiteside JW, Hovan MJ, Engle RL, Edwards FD. Diagnosis and treatment of Lyme disease. *Mayo Clin Proc.* 2008;83(5):566–71.
76. Mogollon-Pasapera E, Otvos L Jr, Giordano A, Cassone M. Bartonella: emerging pathogen or emerging awareness? *Int J Infect Dis.* 2009;13(1):3–8.
77. Pretorius AM, Kelly PJ. An update on human bartonellosis. *Central African J Med.* 2000;46(7):194–200.
78. McElroy KM, Blagburn BL, Breitschwerdt EB, Mead PS, McQuiston JH. Flea-associated zoonotic diseases of cats in the USA: bartonellosis, flea-borne rickettsioses, and plague. *Trends Parasitol.* 2010;26(4):197–204.
79. Ulug M. Evaluation of cat scratch disease cases reported from Turkey between 1996 and 2013 and review of the literature. *Cent Eur J Public Health.* 2015;23(2):170–5.
80. Picascia A, Pagliuca S, Sommese L, et al. Seroprevalence of *Bartonella henselae* in patients awaiting heart transplant in southern Italy. *J Microbiol Immunol Infect.* 2017;50(2):239–44.
81. Maguina C, Guerra H, Ventosilla P. Bartonellosis. *Clin Dermatol.* 2009;27(3):271–80.
82. Batsakis JG, Ro JY, Frauenhoffer EE. Bacillary angiomatosis. *Ann Otol Rhinol Laryngol.* 1995;104(8):668–72.
83. Crocetti D, Palmieri A, Pedulla G, Pasta V, D’Orazi V, Grazi GL. Peliosis hepatis: personal experience and literature review. *World J Gastroenterol.* 2015;21(46):13188–94.

84. DeLeve LD. Vascular liver diseases. *Curr Gastroenterol Rep.* 2003;5(1):63–70.
85. Lezrek O, Laghmari M, Jait A, El Atiqi A, Lezrek M, Daoudi R. Neuroretinitis in ocular bartonellosis. *J Pediatr.* 2015;166(2):496–496.e491.
86. Ormerod LD, Skolnick KA, Menosky MM, Pavan PR, Pon DM. Retinal and choroidal manifestations of cat-scratch disease. *Ophthalmology.* 1998;105(6):1024–31.
87. Biancardi AL, Curi AL. Cat-scratch disease. *Ocul Immunol Inflamm.* 2014;22(2):148–54.
88. Matsuo T, Yamaoka A, Shiraga F, et al. Clinical and angiographic characteristics of retinal manifestations in cat scratch disease. *Jpn J Ophthalmol.* 2000;44(2):182–6.
89. Curi AL, Machado DO, Heringer G, Campos WR, Orefice F. Ocular manifestation of cat-scratch disease in HIV-positive patients. *Am J Ophthalmol.* 2006;141(2):400–1.
90. Gray AV, Reed JB, Wendel RT, Morse LS. Bartonella henselae infection associated with peripapillary angioma, branch retinal artery occlusion, and severe vision loss. *Am J Ophthalmol.* 1999;127(2):223–4.
91. Mason JO III. Retinal and optic nerve neovascularization associated with cat scratch neuroretinitis. *Retina.* 2004;24(1):176–8.
92. Latanza L, Viscogliosi F, Solimeo A, Calabro F, De Angelis V, De Rosa PS. Choroidal neovascularisation as an unusual ophthalmic manifestation of cat-scratch disease in an 8-year-old girl. *Int Ophthalmol.* 2015;35(5):709–16.
93. Manousaridis K, Peter S, Mennel S. Cat-scratch-disease-associated macular oedema treated with intravitreal ranibizumab. *Acta Ophthalmol.* 2015;93(2):e168–70.
94. Empeslidis T, Tsaousis KT, Konidaris V, Pradeep A, Deane J. Multifocal chorioretinitis caused by Bartonella henselae: imaging findings of spectral domain optical coherence tomography during treatment with trimethoprim-sulfamethoxazole. *Eye.* 2014;28(7):907–9.
95. Prutsky G, Domecq JP, Mori L, et al. Treatment outcomes of human bartonellosis: a systematic review and meta-analysis. *Int J Infect Dis.* 2013;17(10):e811–9.
96. Rolain JM, Brouqui P, Koehler JE, Maguina C, Dolan MJ, Raoult D. Recommendations for treatment of human infections caused by Bartonella species. *Antimicrob Agents Chemother.* 2004;48(6):1921–33.